Phenanthrenequinone Adsorbed on Si(001): Geometries, Electronic Properties, and Optical Response

Andreas Hermann,* Wolf G. Schmidt, and Friedhelm Bechstedt

Institut für Festkörpertheorie und-optik, Friedrich-Schiller-Universität Jena, 07743 Jena, Germany

Received: January 3, 2005; In Final Form: February 25, 2005

As a prototypical case of a π-conjugated organic overlayer on a semiconductor surface the adsorption of phenanthrenequinone ($C_{14}O_2H_8$) on the Si(001) surface is studied by means of *first principles* calculations, using gradient-corrected density functional theory together with ultrasoft pseudopotentials and the projector augmented wave method. A thermodynamic phase diagram gives adsorption geometries depending on experimental conditions, the microscopically most favorable bonding configuration representing a "[4+2]-cycloaddition product". The surface electronic structure depends strongly on the respective adsorption configuration. Calculations of the surface optical signature show its sensitivity to molecular adsorption and are in agreement with experimental results. A detailed analysis illustrates that the bonding to the surface has to be taken into account accurately to unveil the molecule's contribution to the surface optical response.

1. Introduction

Organic functionalization of semiconductor surfaces has become a rapidly evolving research branch connecting chemistry and physics at the interface. Possible applications such as chemical or biological sensors[1] or molecular-based electronic circuits[2] stimulate many experimental and theoretical works.[3] For example, the adsorption of small unsaturated hydrocarbons on the Si(001) surface attracts a lot of theoretical interest in order to explore possible bonding configurations.[4−6]

However, π-conjugated organic molecules are of special interest due to their optical and electronic properties:[7] delocalization of the π-electrons shrinks the gap leading to semiconducting rather than insulating behavior. Exploiting this property in an adsorbed organic layer incorporates the need for the π-conjugation to remain intact upon adsorption.[8]

The adsorption of phenanthrenequinone ("PQ", $C_{14}O_2H_8$) on Si(001) serves as a prototypical process of semiconductor functionalization. It was investigated by various experimental techniques probing structural, electronic, and optical properties of the adsorbed layer.[9,10] Scanning Tunneling Microscopy and X-ray Photoemission Spectroscopy together with Fourier Transform Infrared Spectroscopy led to the conclusion that (i) PQ adsorption is a self-terminating process leading to an ordered (sub-) monolayer coverage, (ii) PQ bonds to the substrate via both of its carbonyl groups forming Si−O−C bonds, (iii) the remaining C atoms are not involved in bonding, and (iv) the π-conjugated electron system remains intact. Since they provide additional information about the electronic structure, optical spectroscopic methods might be useful in characterizing organic thin films. However, a surface sensitive method is needed to suppress the dominant optical signal of the underlying substrate material. Reflectance Anisotropy Spectroscopy (RAS) fulfills this condition and is known as a valuable tool in characterizing clean and atom-adsorbed semiconductor surfaces:[11] the relative difference in reflectivity is measured for normally incident light linearly polarized along the surface crystal axes, depending on the frequency of the incident light. Since the substrate is optically isotropic, the measured signal depends only on the surface properties.

In this article we present results of a comprehensive *first principles* study on the adsorption of PQ on Si(001). We discuss the thermodynamically most favorable adsorption configurations, the electronic and optical properties of the thin PQ-films, in comparison with experimental findings. We show that both electronic and optical properties depend strongly on the specific adsorption configuration. A detailed analysis is presented to single out intramolecular contributions to the optical spectra.

2. Method

For electronic ground-state calculations we employ gradient-corrected density functional theory (DFT-GGA)[12,13] as implemented in the Vienna Ab initio Simulation Package,[14] using the PW91 exchange-correlation functional[15] and a plane wave basis set. Ionic relaxations are performed by using conjugate-gradient or quasi-Newton algorithms to minimize the Hellmann−Feynman forces. We consider a structure to be in equilibrium if each Cartesian component of the atomic forces falls below 10 meV/Å.

The electron−ion interaction is modeled by means of norm-conserving ultrasoft pseudopotentials[16] allowing for accurate treatment of first-row elements already with relatively small basis sets. We expand the wave functions into plane waves up to a cutoff energy of 25 Ry, which previous studies have shown to be sufficient in treating small molecules on surfaces.[17,18]

The surface region is modeled within the periodically repeated slab approach. For structural relaxations we use an 8-layer asymmetric Si slab, the bottom of which is saturated with hydrogen. The upper five Si layers and the adsorbates are allowed to relax, while the three lowest Si layers are kept fixed in their bulk positions. Two slabs are separated by an equivalent of 12 Si layers of vacuum to avoid direct interaction of neighboring surfaces through the vacuum. The electrostatic dipole moment of the slab is compensated by a suitable dipole area density in the middle of the vacuum region, so that the net dipole moment of the slab is zero. Brillouin zone integrations

* Address correspondence to this author. E-mail: hermann@ifto.physik.uni-jena.de.

10.1021/jp0500182 CCC: $30.25
Published on Web 03/30/2005

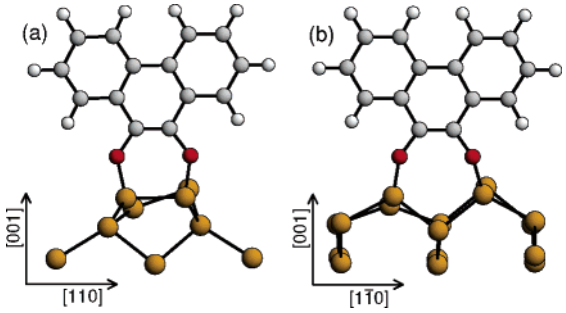

Figure 1. Possible adsorption geometries for PQ on Si(001): (a) top dimer (TD) and (b) cross dimer (CD). Red (gray, white, brown) circles denote O (C, H, Si) atoms, from ref 31.

are performed on regular meshes in reciprocal space,[19] corresponding to 64 k points in the (1 × 1) surface Brillouin zone.

For optical properties we construct a 12-layer symmetric slab out of the relaxed structure and calculate transition matrix elements from all-electron wave functions using the Projector Augmented Wave method[20,21] and an equivalent of 256 k points in the (1 × 1) surface Brillouin zone. The diagonal components of the dielectric tensor $\epsilon_{ii}(\omega)$ are then calculated in independent particle approximation, but applying a scissors operator shift of $\Delta E = 0.50$ eV to account for the DFT-GGA band gap underestimation. The RAS signal is given by[22]

$$\frac{\Delta r}{r}(\omega) = \frac{2\omega}{d}\,\mathrm{Im}\left\{\frac{\Delta\epsilon_{ii}(\omega)}{\epsilon_{\mathrm{b}}(\omega) - 1}\right\} \qquad (1)$$

where d is the slab thickness and $\epsilon_{\mathrm{b}}(\omega)$ is the bulk dielectric function of Si.

3. Results and Discussion

3.1. Structural Properties. The Si(001) surface atoms are known to form tilted dimers, the low-temperature ground state having $c(4 \times 2)$ symmetry.[23,24] The adsorption geometry of PQ on this surface was thoroughly investigated by Hamers et al.[9] Starting from their findings several bonding models can be proposed. The most relevant ones are shown in Figure 1: the top dimer model (TD), where PQ bonds to one underlying Si dimer, and the cross dimer model (CD), where PQ connects two dimers within one dimer row. Another possibility would be PQ connecting two dimers of adjacent rows, which we call the bridge dimer model (BD). Mind that in CD the molecule is rotated by 90° with respect to TD. The TD geometry might be called a "cycloaddition product" due to its formal analogy to the product of a heteroatomic Diels−Alder or [4+2]-cycloaddition reaction.[3]

To model the initial stage of PQ adsorption on the clean surface we assume PQ to be already bound to an electrophilic "down"-dimer atom via one carbonyl group. It is known that the reaction barrier for the formation of such a dative bond is rather low.[25] Keeping the binding O atom fixed, we calculate the total energies for various tilting angles θ (between the surface normal and the molecular principal axis) and rotation angles ϕ (between the dimer direction and the molecular plane). The inset of Figure 2 shows a schematic top view of how ϕ is oriented. Mind that $\phi = 0°$ (90°, 180°) corresponds to TD (CD, BD) geometry, if $\theta = 0°$. To avoid interactions between the tilted and rotated PQs in neighbored supercells we must use a $p(4 \times 4)$ surface supercell. We calculate the energy difference

$$\Delta E_{\mathrm{ads}} = E^{\mathrm{PQ}}_{\mathrm{slab}} - E^{\mathrm{clean}}_{\mathrm{slab}} - E^{\mathrm{PQ}}_{\mathrm{gas\ phase}} \qquad (2)$$

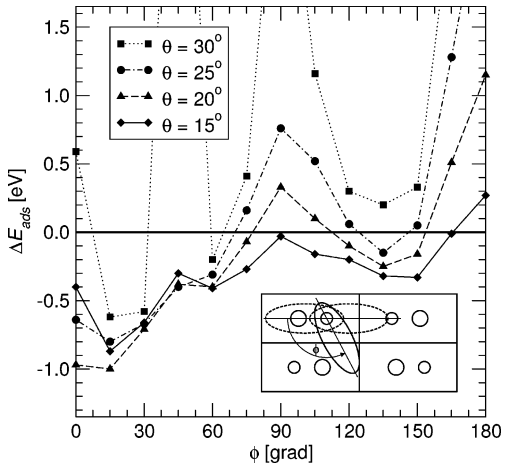

Figure 2. Initial sticking process of PQ on Si(001): adsorption energies for various tilting angles θ via rotation angle ϕ. The inset shows the definition of rotation angle ϕ.

while keeping the geometries of the surface as well as the PQ molecule fixed; structural relaxation of such a large supercell is on one hand numerically hardly affordable and on the other hand would possibly spoil the usefulness of the parameter set (θ,ϕ) since these might change during the relaxation process. The results of our calculations are compiled in Figure 2. Over the entire range of ϕ, the energy ΔE_{ads} is lowered by lowering the tilting angle θ, thus no significant barrier exists for establishing a bond between the second O atom and the surface. The only exception is $\phi = 0°$, where decreasing θ below the dimer tilting angle (which is $\theta_d = 18.7°$ in our calculation) results in stronger repulsion between PQ and the surface. Local minima at $\phi = 60°$, 135° result from the frozen geometry ansatz leading to steric repulsion if PQ is oriented parallel or perpendicular to the dimers. They do not lead to global energy minima since structural relaxation gives a much higher energy gain for the double bonded molecules (see below). However, qualitatively TD is preferred over CD which is preferred over BD for every angle θ. It turns out that this relation holds also after structural relaxation.

We calculate the relaxed ground state and its energy of more than 20 conceivable adsorption patterns by combining one or more of the aforementioned geometries in a $p(4 \times 2)$ surface supercell. Among them we consider the possible coadsorption of atomic hydrogen saturating unoccupied Si dimer atoms. To compare configurations of different coverage one has to minimize the grand canonical potential Ω of the slab, or, equivalently, the surface free energy $\gamma \equiv \Omega/A$ depending on the chemical potentials μ_{H}, μ_{PQ} of the adsorbates H and PQ (where the Si chemical potential is fixed to its bulk value $\mu^{\mathrm{bulk}}_{\mathrm{Si}}$):[26,27]

$$\gamma = \frac{1}{A}\left[E^{\mathrm{tot}}_{\mathrm{slab}} - N_{\mathrm{PQ}}E^{\mathrm{PQ}}_{\mathrm{gas\ phase}} - \frac{N_{\mathrm{H}}}{2}E^{\mathrm{H_2}}_{\mathrm{gas\ phase}}\right] - \frac{N_{\mathrm{PQ}}}{A}\Delta\mu_{\mathrm{PQ}} - \frac{N_{\mathrm{H}}}{A}\Delta\mu_{\mathrm{H}} \qquad (3)$$

where $N_{\mathrm{H/PQ}}$ gives the number of H/PQ adsorbed in the surface cell of area A and $E^{\mathrm{tot}}_{\mathrm{slab}}$ gives the total slab energy of the respective configuration. We treat H and PQ as independent chemical components thereby neglecting any reactions between them.

The resulting phase diagram is shown in Figure 3. For each point in the two-dimensional $(\Delta\mu_{\mathrm{H}}, \Delta\mu_{\mathrm{PQ}})$ space the configuration that minimizes expression 3 is given. The values $\Delta\mu_{\mathrm{H}} =$

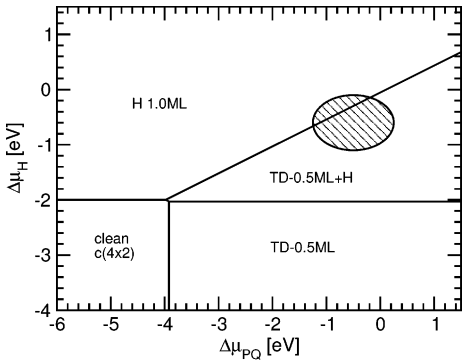

Figure 3. 2D phase diagram with the most relevant area of preparation conditions marked by a hatched circle.

0 ($\Delta\mu_{PQ} = 0$) correspond to H-rich (PQ-rich) conditions. We assume the experimentally relevant region to be well described by $\Delta\mu_{PQ} \approx -1, ..., 0$ eV, $\Delta\mu_H \approx -1, ..., -0.5$ eV. Under these conditions the thermodynamically most favored adsorption configuration is TD-0.5ML+H. It is comprised of 0.5 monolayer (ML) of PQ coverage (i.e. one PQ molecule per two Si dimers), where the PQ molecules (each bonding in TD geometry) are staggered on the surface, and hydrogen is saturating the remaining Si dimer atoms (see Figure 4d for molecular arrangement). The most favored non-TD configuration under these chemical conditions is CD-0.5ML+H. It has the same surface stoichiometry: the PQ molecules bond in CD geometry in 0.5 ML coverage in staggered arrangement, and hydrogen saturates the remaining Si dimer atoms. However, PQ bonding in TD is favored over CD by about 0.24 eV per molecule. Full ML PQ coverage is not favored over the entire range of $\Delta\mu_{PQ}$ considered because of steric repulsion of the molecules outweighing the energy gain of the bonding process.

3.2. Electronic Structure. The clean Si(001)$-c(4 \times 2)$ surface is semiconducting, with a band gap of about 0.3 eV in standard DFT calculations.[28] The Si surface atoms form alternately tilted asymmetric dimers. The formation of an asymmetric dimer results in a charge transfer from the "down"-dimer to the "up"-dimer atom. Thus the highest occupied clean surface state is an s-like orbital localized at the "up"-dimer atom and the lowest unoccupied state is a p-like orbital at the "down"-dimer atom.[18,23] Since the latter is more delocalized, the bandwidth of the lowest conduction bands is larger than those of the highest valence bands. The interaction between the orbitals along the dimer rows is stronger than that between adjacent dimer rows.

Molecular adsorption processes might change these surface electronic properties drastically, depending on the details of the adsorption.[18,29] In Figure 4 calculated surface band structures of several PQ adsorption configurations are compiled, together with charge density isosurface plots of the highest occupied (HOMO) and lowest unoccupied molecular orbitals (LUMO) in the $p(4 \times 2)$ surface cell. The shaded area in the plots indicates the projected Si bulk band structure.

In TD-0.25ML configuration (see Figure 4a) one PQ molecule is bound to one Si dimer in the surface cell. The occupied and unoccupied dimer states of the underlying dimer are removed from the surface band structure. The new HOMO is an orbital localized at PQ, more precisely it is mainly a C=C π-bond, the formation of which results from the [4+2]-cycladdition. It belongs to an almost completely flat band; due to spatial separation the interaction with other surface states is strongly reduced. However, the saturation of the underlying dimer's dangling bonds and the accompanying structural reconfiguration influence the remaining surface states in the unit cell. The occupied state of the neighboring dimer within the same dimer row is shifted to lower energy, whereas the unoccupied state localized at the same dimer is shifted to higher energy. Since the interaction between dimer rows remains weak even after adsorption, the occupied and unoccupied states of the dimers in the adjacent dimer row remain almost unchanged. The dispersion of the respective bands is found to agree with calculations of the clean surface. The LUMO thus resides at the "down"-atom of the nearest Si dimer in the adjacent dimer row. Since the highest occupied state localized at PQ is close to the bulk valence band maximum, the surface remains semiconducting.

This changes in the TD-0.5ML-a configuration, where two PQ molecules are aligned in the surface cell (see Figure 4b). The HOMO at k point K is degenerated and formed by a linear combination of the C=C π-bonds of the PQ molecules. Since these interact strongly along the dimer rows, a splitting of the corresponding bands occurs along $\Gamma-J'$ and the degeneracy is broken at Γ. However, the dimer states of the adjacent row remain mainly unchanged and therefore a band crossing between the nonbonding HOMO and the unoccupied dimer states occurs

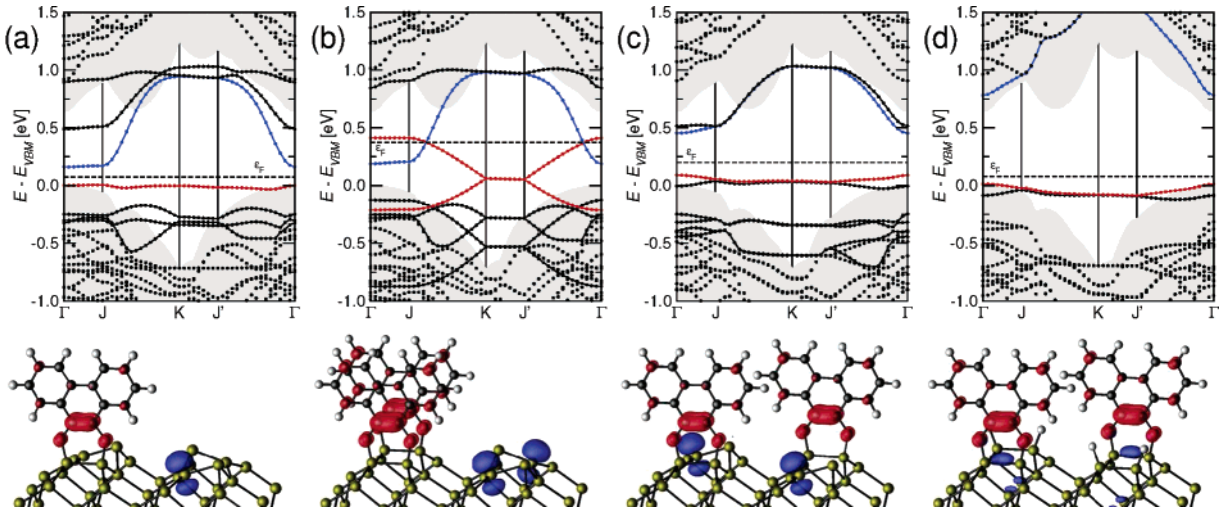

Figure 4. (a) TD-0.25ML, (b) TD-0.5ML-a (aligned), (c) TD-0.5ML-s (staggered), and (d) TD-0.5ML+H (with hydrogen). Upper panel: surface band structures of configurations. Lower panel: charge density isosurface ($\rho = 0.06$ e/Å^3) for respective HOMO (red) and LUMO (blue) at the K point of the surface Brillouin zone.

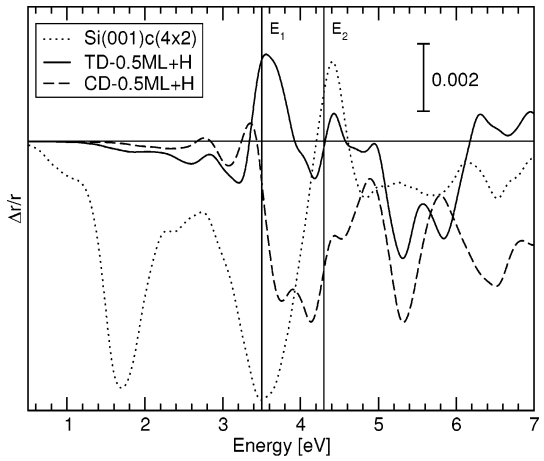

Figure 5. $\Delta r/r = \mathrm{Re}\{(r_{110} - r_{1\bar{1}0})/\langle r\rangle\}$ for the clean surface and two most relevant PQ adsorption configurations.

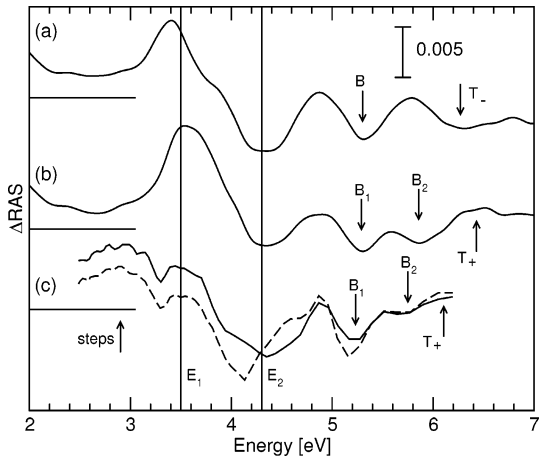

Figure 6. Comparison of calculated ΔRAS with experimental data: (a) calculation CD-0.5ML+H, (b) calculation TD-0.5ML+H, and (c) experiment for exposure of 0.1 L (solid line) and 1.3 L (dashed line), enhanced by a factor of 3. Clean surface spectra are subtracted.

at about 0.2 Γ−J′. Thus the surface becomes metallic along the dimer rows, having electrons injected from the HOMO localized at PQ into dimer states. Existing ultraviolet photoemission spectroscopy measurements[10] concentrate on the anisotropy of the valence-band photoemission rather than on its properties near the Fermi energy level, thus no experimental statement on surface metallicity is available.

If PQ molecules are arranged in a staggered configuration in the surface cell, one obtains the TD-0.5ML-s configuration (see Figure 4c). The surface has $c(4 \times 2)$ symmetry, thus bands should be degenerated along J−K−J′, which is fairly well fulfilled. The HOMO at K is again formed by a linear combination of C═C π-bonds. Their interaction is, however, rather weak, therefore the bandwidth is small. The occupied and unoccupied free dimer states are shifted in a way similar to the TD-0.25ML configuration to lower and higher energies, respectively, their bandwidth being reduced. The LUMO is formed by a combination of unoccupied free dimer states. Since there is only a little interaction between the PQ molecules, the surface remains semiconducting. This is the most favored configuration in case no hydrogen is available.

If the remaining dimers are saturated with hydrogen, as is the case in the TD-0.5ML+H configuration shown in Figure 4d, the dimer states are completely removed from the gap, and only the HOMO localized at PQ remains. The LUMO is shifted to much higher energies and changes its character drastically. It is much more delocalized and mixes with bulklike states. Therefore the isosurface value in the charge density plot is lowered to $\rho = 0.01$ e/Å^3 for this state compared to $\rho = 0.06$ e/Å^3 for all other shown orbitals. It can be seen that the LUMO (at least at K) is "mostly localized" directly beneath the PQ molecules having Si═Si π*-bond character.

3.3. Optical Properties. Hamers et al. studied the optical properties of thin PQ layers on Si(001).[10] Since PQ is known to form ordered monolayers in a self-terminating adsorption process under conservation of the π-conjugated electron system, the reflectance anisotropy of the adsorbate-covered surface should be modified due to the strongly anisotropic intramolecular $\pi-\pi$* transitions. Since the lowest such transitions are known to appear at about $E = 4$ eV, they should be visible in a standard RAS experiment normally covering an energy range of 2−6 eV.

The calculated RAS spectra for the two favored configurations discussed in subsection 3.1 are given in Figure 5, together with the calculated RAS spectrum of the clean Si(001)-$c(4 \times 2)$ surface. For clarity the spectral positions of the bulk critical points (CPs) $E_{1/2}$ are indicated by vertical lines. Irrespective of the specific configuration, the 1.7 eV feature of the clean surface vanishes upon adsorption. This can be explained, since it is known to be related to free dimer state interaction and all dimer states are removed in these configurations. The pronounced features at the CPs E_1 and E_2 are modified depending strongly on the details of the adsorption. A pronounced negative feature at 5.3 eV shows up in both configurations.

Experimental results are shown in Figure 6c, for two different exposures of PQ to the substrate. The measured RAS signal of the clean Si(001) surface is subtracted to emphasize adsorption induced effects. Both spectra are rather similar in line shape and amplitude, thus indicating that the PQ adsorption process is completed already after relatively low exposure. A broad maximum at low energies (below 3 eV) may be related to the fact that stepped surfaces were used in experiment, which are known to influence the RAS signal in this spectral region.[30] Features near the CPs E_1 and E_2 indicate the modification of bulklike wave functions in the near-surface region upon PQ adsorption. At higher energies a significant negative feature B_1 at $E = 5.2$ eV is reported, followed by a rather small dip B_2 at $E = 5.7$ eV and a positive energy trend T_+ above 6 eV. Experimentalists attributed the feature B_1 to intramolecular $\pi-\pi$* transitions. This conclusion was substantiated by the fact that similar experiments on the adsorption of the single-ringed molecule 1,2-cyclohexanedione ("CHD", $C_6O_2H_8$) on Si(001), which is likely to proceed in the same manner via the carbonyl groups, did not yield such a feature. However, our calculations indicate that the conclusion may be questionable: we find a negative feature at 5.3 eV in both spectra shown in Figure 5 but, as the PQ molecules are rotated by 90° with respect to another in TD and CD geometry, a $\pi-\pi$* transition related RAS feature should change its sign in the two spectra. Such a mirrorlike behavior can be found only near CP E_1 and at high energies above 6 eV.

To compare the calculations directly with experimental data, we subtract the calculated signal of the clean surface; the results are given in Figure 6a,b. As expected, the low energy step-related feature is not reproduced. However, the positive and negative modifications near the CPs E_1 and E_2 are reproduced by both configurations. Although the RAS signals are quite different, after subtraction of the clean surface RAS signal the line shape is rather similar with only little variation in peak position and amplitude. So, independent of the details of the adsorption, the pure existence of adsorbates on the surface

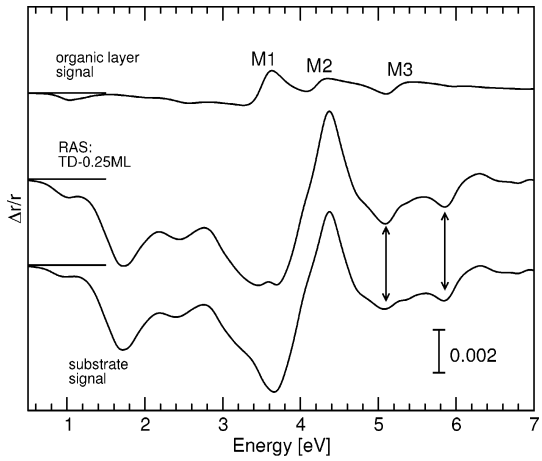

Figure 7. Decomposition of the RAS signal of the TD-0.25ML configuration into the organic layer and substrate contributions.

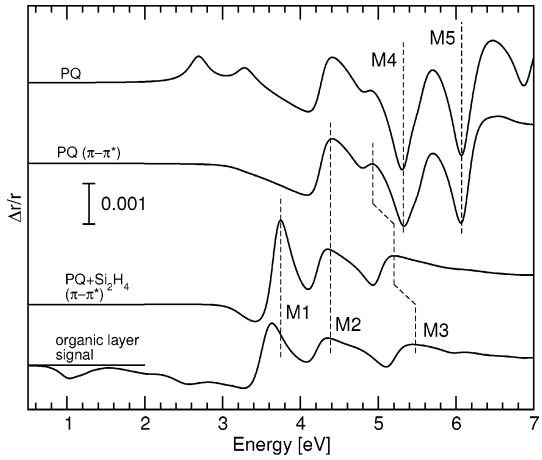

Figure 8. RAS of several cluster models (see text) and organic layer signal of the TD-0.25ML configuration.

changes the E_1 and E_2 peaks in a more or less similar way, including reduction and even inversion of the respective signals. At higher energies differences between the configurations can be noticed more clearly. The B_1 and B_2 feature as well as the energy trend T_+ can be found in the TD-0.5ML+H spectrum. On the other hand, the CD-0.5ML+H spectrum shows a single negative feature B and a negative energy trend T_- above 6 eV. Again, a negative feature near 5.2 eV occurs in both configurations, making its origin in $\pi-\pi^*$ transitions questionable. The spectrum of the TD configuration agrees better with experiment than that of the CD configuration, thus coinciding with the discussion of the total energies given above. Moreover, the overall good agreement of the calculated spectrum with experiment encourages us to further investigate the origin of the respective peaks and especially try to identify the anisotropic $\pi-\pi^*$ transitions within the spectra.

3.4. Analysis of RAS Features. Since the π-conjugated electron system remains intact upon adsorption, for sure some anisotropic intramolecular transitions must exist, likely to influence the RAS signal. However, they could not be derived from the calculated spectra so far. To achieve this goal, we perform a "state-by-state" decomposition of the set of valence orbitals with respect to the localization of each orbital above or below the Si surface. This allows for the calculation of two different contributions to the total RAS signal, stemming from the organic layer and the substrate region, repectively. The organic layer contribution should be composed by intra- or intermolecular transitions, only, and thus help to identify and quantify the molecular influence on the surface optical response. The decomposition benefits from the size of the molecule and its standing upright on the surface, thereby spatially separating the interesting π-electron system from the substrate region and allowing for application of a meaningful localization condition.

For the remainder of this paragraph we discuss as an exemplary case the TD-0.25ML configuration. A discussion of the TD-0.50ML+H configuration has been published elsewhere.[31] In Figure 7 the total RAS signal of this configuration and its decomposition obtained as described above are shown. The total spectrum does not differ very much from the clean surface spectrum, since the PQ coverage is low. The 1.7 eV feature is decreased by a factor of 2, because of the PQ molecules preventing free dimer state interaction in every second dimer row. However, the organic layer signal constitutes three remarkable peaks at 3.6, 4.3, and 5.3 eV, named M1−M3, respectively. Once again, the 5.3 eV and the 5.8 eV features do not stem from organic layer transitions.

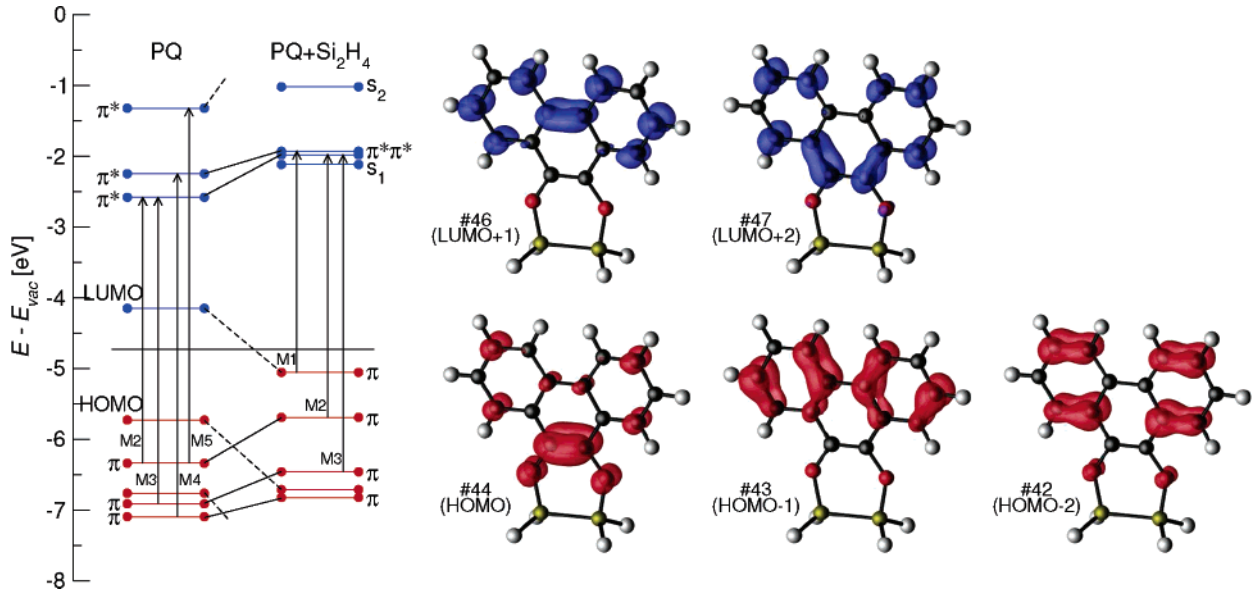

Figure 9. Left: Shift of PQ orbitals and intramolecular transitions upon binding to Si_2H_4 cluster. Right: charge density isosurface plots of occupied and unoccupied orbitals of PQ+Si_2H_4 involved in transitions M1−M3.

The significant peaks M1−M3 must be related to some $\pi-\pi^*$ transitions. To identify these we introduce a simple 3-layer model consisting of the optically isotropic bulk material (here Si), an optically anisotropic organic layer, and a vacuum. The slab dielectric tensor components entering the RAS formula (1) are approximated by gas-phase dielectric functions of appropriate clusters or molecules, normalized to the area density of 0.25 ML. We thereby model the organic thin film by a fictitious layer of noninteracting gas-phase-like responding molecules or clusters. The results we obtain for the different "thin film constituents" are compiled in Figure 8.

In a first step we use the gas-phase dielectric function of the PQ molecule. Its diagonal components $\epsilon_{xx}^{PQ}(\omega)$, $\epsilon_{yy}^{PQ}(\omega)$ (where x, y are perpendicular to the molecular principal axis along z) are calculated in independent particle approximation, but applying a scissors operator shift of 0.5 eV to be comparable to the slab calculations. Fortunately a ΔSCF calculation with occupation constraint shows that the molecular optical gap opens up by about the same value with respect to the DFT gap. Calculating the reflectance anisotropy of a single PQ molecule and normalizing to 0.25 ML coverage on Si(001) yields the uppermost curve in Figure 8 Comparison with the organic layer signal (given as the lowest curve in Figure 8) shows very poor agreement.

In a second step we restrict the PQ dielectric function to only $\pi-\pi^*$ transitions, yielding the second curve in Figure 8. Since PQ bonds to the substrate via its carbonyl groups, all carbonyl-localized transitions of the gas-phase molecule should be shifted to much higher energies. Thus, taking into account only the $\pi-\pi^*$ transitions should improve agreement with the organic layer signal. Indeed, agreement in the low energy region is slightly better; however, the significant features M4 and M5 are still present, but cannot be found in the organic layer signal.

In a third step we construct a PQ+Si_2H_4 cluster, where PQ binds via the carbonyls to a hydrogen-saturated Si dimer, to take into account the bonding to the substrate more accurately. Calculating the dielectric function of that cluster and restricting it to $\pi-\pi^*$ transitions within the PQ only, we obtain the third curve in Figure 8. It matches the organic layer signal very well concerning peak positions and amplitudes. This finally shows that the latter stems from $\pi-\pi^*$ transitions which are, however, strongly modified by the bonding to the substrate. With the cluster model at hand we can identify the specific transitions responsible for the features M1−M3.

In the left part of Figure 9 the energy shifts of the highest occupied and lowest unoccupied orbitals when going from the free PQ molecule to the PQ+Si_2H_4 cluster are shown. The significant features M1−M5 of Figure 8 are also plotted as intramolecular transitions. The correspondence between the PQ gas-phase orbitals and the PQ+Si_2H_4 cluster orbitals is reached by comparing the respective charge density distributions. In the right part of Figure 9 these charge density distributions are given for the orbitals of the PQ+Si_2H_4 cluster involved in transitions M1−M3. Upon bonding to the Si dimer, the PQ LUMO, which is mainly the C═C double bond of the carbonyls' C atoms, becomes populated and forms the new PQ+Si_2H_4-HOMO; the PQ's π- and π^*-orbitals are shifted upward and two new Si═Si bond localized unoccupied states s_1 and s_2 show up. The transition M1 appears only due to formation of the new HOMO, the transitions M2 and M3 are shifted in energy, and M4 and M5 disappear by losing almost all of their oscillator strength.

The optical anisotropy of adsorbed PQ molecules can thus be traced back to three dominant intramolecular transitions; although seemingly spatially decoupled, the interaction between the "bonding" carbonyl groups and the "functional" π-electron system leads to reasonably altered optical properties after adsorption on the substrate.

4. Summary

The adsorption of phenanthrenequinone on Si(001) was studied using *first principles* calculations. The most favored adsorption configurations were given, depending on the experimental conditions. The electronic structure as well as the optical signature of the adsorbed surfaces were shown to be strongly dependent on the microscopic details of the adsorption. The calculated optical spectra are in good agreement with experimental data. However, it is shown that a simplified interpretation of optical signatures in terms of gas-phase absorption spectra may be unreliably and possibly leads to wrong conclusions.

Acknowledgment. Grants of computer time from the Leibniz-Rechenzentrum München and the Höchstleistungsrechenzentrum Stuttgart are gratefully acknowledged. We thank the Deutsche Forschungsgemeinschaft for financial support (SCHM-1361/6).

References and Notes

(1) Yates, J. T., Jr. *Science* **1998**, *279*, 335−336.
(2) Joachim, C.; Gimzewski, J. K.; Aviram, A. *Nature* **2000**, *408*, 541−548.
(3) Bent, S. F. *Surf. Sci.* **2002**, *500*, 879−903.
(4) Miotto, R.; Ferraz, A. C.; Srivastava, G. P. *Phys. Rev. B* **2001**, *65*, 075401.
(5) Silvestrelli, P. L.; Pulci, O.; Palummo, M.; Del Sole, R.; Ancilotto, F. *Phys. Rev. B* **2003**, *68*, 235306.
(6) Cho, J.-H.; Kleinman, L. *Phys. Rev. B* **2004**, *69*, 075303.
(7) Friend, R. H.; Gymer, R. W.; Holmes, A. B.; Burroughes, J. H.; Marks, R. N.; Taliani, C.; Bradley, D. D. C.; Dos Santos, D. A.; Brédas, J. L.; Lögdlund, M.; Salaneck, W. R. *Nature* **1999**, *397*, 121−128.
(8) Hamers, R. J. *Nature* **2001**, *412*, 489−490.
(9) Fang, L.; Liu, J.; Coulter, S.; Cao, X.; Schwartz, M. P.; Hacker, C.; Hamers, R. J. *Surf. Sci.* **2002**, *514*, 362−375.
(10) Hacker, C. A.; Hamers, R. J. *J. Phys. Chem. B* **2003**, *107*, 7689−7695.
(11) Schmidt, W. G.; Seino, K.; Hahn, P. H.; Bechstedt, F.; Lu, W.; Wang, S.; Bernholc, J. *Thin Solid Films* **2003**, *455/456*, 764−771.
(12) Hohenberg, P.; Kohn, W. *Phys. Rev.* **1964**, *136*, B864−B871.
(13) Kohn, W.; Sham, L. *Phys. Rev.* **1965**, *140*, A1133−A1138.
(14) Kresse, G.; Furthmüller, J. *Phys. Rev. B* **1996**, *54*, 11169−11186.
(15) Perdew, J. P.; Chevary, J. A.; Vosko, S. H.; Jackson, K. A.; Pederson, M. R.; Singh, D. J.; Fiolhais, C. *Phys. Rev. B* **1992**, *46*, 6671−6687.
(16) Vanderbilt, D. *Phys. Rev. B Rapid Commun.* **1990**, *41*, 7892−7895.
(17) Seino, K.; Schmidt, W. G.; Preuss, M.; Bechstedt, F. *J. Phys. Chem. B* **2003**, *107*, 5031−5035.
(18) Preuss, M.; Schmidt, W. G.; Bechstedt, F. *J. Phys. Chem. B* **2004**, *108*, 7809−7813.
(19) Monkhorst, H. J.; Pack, J. D. *Phys. Rev. B* **1976**, *13*, 5188−5192.
(20) Blöchl, P. E. *Phys. Rev. B* **1994**, *50*, 17953−17979.
(21) Kresse, G.; Joubert, D. *Phys. Rev. B* **1999**, *59*, 1758−1775.
(22) Del Sole, R. *Solid State Commun.* **1981**, *37*, 537−540.
(23) Krüger, P.; Pollmann, J. *Phys. Rev. Lett.* **1995**, *74* (7), 1155−1158.
(24) Seino, K.; Schmidt, W. G.; Bechstedt, F. *Phys. Rev. Lett.* **2004**, *93*, 036101.
(25) Wang, G. T.; Mui, C.; Musgrave, C. B.; Bent, S. F. *J. Am. Chem. Soc.* **2002**, *124*, 8990−9004.
(26) Qian, G.-X.; Martin, R. M.; Chadi, D. J. *Phys. Rev. Lett.* **1988**, *60*, 1962−1965.
(27) Esser, N.; Shkrebtii, A. I.; Resch-Esser, U.; Springer, C.; Richter, W.; Schmidt, W. G.; Bechstedt, F.; Del Sole, R. *Phys. Rev. Lett.* **1996**, *77*, 4402.
(28) Ramstad, A.; Brocks, G.; Kelly, P. J. *Phys. Rev. B* **1995**, *51*, 14504−14523.
(29) Seino, K.; Schmidt, W. G.; Bechstedt, F. *Phys. Rev. B* **2004**, *69*, 245309.
(30) Schmidt, W. G.; Bechstedt, F.; Bernholc, J. *Phys. Rev. B* **2001**, *63*, 045322.
(31) Hermann, A.; Schmidt, W. G.; Bechstedt, F. *Phys. Rev. B.* Accepted for publication.